PCCP

Accepted Manuscript

ROYAL SOCIETY OF CHEMISTRY

www.rsc.org/pccp

Physical Chemistry Chemical Physics

ARTICLE

Formation Mechanism and yield of small Imidazoles from Reactions of Glyoxal with NH_4^+ in water at neutral pH

Received 00th May 2015,
Accepted 00th January 20xx

DOI: 10.1039/x0xx00000x

www.rsc.org/

A. Maxut,[a] B. Nozière,[a,*] B. Fenet,[b] and H. Mechakra[a,c]

Imidazoles have numerous applications in pharmacology, chemistry, optics and electronics, making it worthwhile the development of environmentally-friendly synthetic procedures. In this work, the formation of imidazole, imidazole-2-carboxaldehyde, and 2,2-bis-1H-imidazole was investigated in the self-reaction of glyoxal and its cross-reactions with each of these compounds in aqueous solutions of inorganic ammonium salts at pH = 7. Such conditions are relevant both as cheap and environmentally-friendly synthetic procedures and for the chemistry of natural environments where NH_4^+ is abundant, such as atmospheric aerosols. These reactions were investigated both by ^{1}H-NMR and UV-Vis absorption spectroscopy at room temperature and the objective was to determine the formation pathways for the three imidazoles and the parameters affecting their yields, to identify the optimal conditions for their synthesis. The results show that only the simplest imidazole is produced in the self-reaction of glyoxal and that imidazole-2-carboxaldehyde and 2,2-bis-1H-imidazole are produced by its cross-reactions with imidazole and imidazole-2-carboxaldehyde, respectively. The yields for imidazole-2-carboxaldehyde and 2,2-bisimidazole in the cross-reactions were close to unity, but the one for imidazole in the self-reaction of glyoxal, Y_{Im}, was small and varied inversely with glyoxal initial concentration, $[G]_o$: Y_{Im} > 10 % only for $[G]_o$ < 0.1 M. This later result was attributed to the kinetic competition between the imidazole-forming condensation pathway and the acetal/oligomer formation pathway of the glyoxal self-reaction, and constitutes a bottleneck for the formation of higher imidazoles. Other parameters such as pH and NH_4^+ concentration did not affect the yields. Thus, by maintaining small glyoxal concentrations, high imidazole yields can be achieved in environmentally-friendly aqueous ammonium solutions at neutral pH. Under the same conditions, better yields are also expected from substituted carbonyl compounds, regardless of their concentration, as they produce less acetals.

Introduction,

Imidazoles have countless applications in pharmacology,[1, 2] chemistry,[3-5] and optics and electronics.[6-9] These numerous applications make it worthwhile the identification of cheap and environmentally friendly synthetic procedures for these compounds. Many of the procedures employed, especially to produce non-alkylated imidazole rings, start from glyoxal.[10-14] The classical methods employ ammonia as co-reagent[10-12] but result in moderate molar yields. More recent methods have replaced NH_3 by its aqueous counterpart, NH_4OH[13, 14] or an inorganic ammonium salts combined with a strongly alkaline element[14] (generally a metal hydroxide) and moderate temperature (30-60 °C), leading to better yields. In the last few years, the formation of imidazole (Im),[15-17] imidazole-2-carboxaldehyde (IC),[15-17] and 2,2-bis-1H-imidazole (BI)[17] (Figure 1) in the reactions of glyoxal (G) with more neutral inorganic ammonium salts, such as $(NH_4)_2SO_4$, in water and at room temperature, was demonstrated.[15, 16, 18] Such reaction conditions are relevant in atmospheric aerosols, where NH_4^+ is abundant ($[NH_4^+]$ >> 1 M) and provide also environmentally-friendly alternatives for the synthesis of imidazoles. The kinetics of the self-reaction of glyoxal under these conditions has been extensively studied[16, 18, 19] but the formation mechanisms and yields for the imidazoles were not established. These yields were, however, estimated to be small.

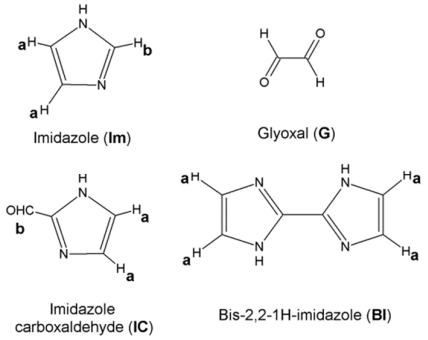

Figure 1: Structures of the compounds investigated in this work.

[a] Institut de Recherches sur la Catalyse et l'Environnement de Lyon (IRCELYON), CNRS and Université Lyon 1, 69626 Villeurbanne, France.
[b] Centre Commun de RMN (CCRMN), Université de Lyon 1 and Ecole Supérieure de Chimie, Physique, Electronique de Lyon (CPE), 69626 Villeurbanne, France.
[c] Now at Laboratoire des Sciences et Technologie de l'Environnement (LSTE), Université des Frères Mentouri Constantine, Algeria.
* corresponding author. Email: barbara.noziere@ircelyon.univ-lyon1.fr, Tel: (+33) 427465732

This work further investigates the formation of these imidazoles from glyoxal in aqueous ammonium salt solutions, with the objective to determine if the production of significant yields under neutral and aqueous conditions is possible and, if so, their optimal conditions. For this, experiments were performed in order to 1) elucidate the formation pathways for Im, IC and BI, 2) quantify their yields, and 3) identify the experimental parameters affecting these yields.

Experimental

All the reactions studied in this work were investigated both by ^{1}H-NMR and UV-Vis absorption spectroscopy, and at room temperature (298 ± 2) K. The imidazoles produced were identified by ^{1}H-NMR and their yields determined by both techniques for consistency. The experiments were performed in 2 - 4 mL glass vials, protected from light and continuously stirred over the entire duration of the experiment. In all the experiments, the precursors for NH_4^+ was ammonium sulfate, $(NH_4)_2SO_4$, at a concentration of 0.1 M, either in H_20 for the UV-Vis studies or in D_2O for the ^{1}H-NMR ones. Previous studies of the self-reaction of gloxal,[18] have shown that other ammonium salts had identical effects on the reaction. The experiments performed in this work and their conditions are summarized in Table 1. In addition to these experiments, a series of about 70 experiments previously used for a kinetic study of the self-reaction of glyoxal in aqueous ammonium salt solutions by UV-Vis absorption[18] were re-analyzed to determine the imidazole yield over a wider range of conditions: initial concentration of G, $[G]_o$, between 0.1 and 0.5 M, $[(NH_4)_2SO_4]$ = 1.9 – 6 M, pH = 5 - 9. In this paper, the effects of NH_4^+ on the kinetics and yields are discussed in term of NH_4^+ activity, a_{NH4+}, rather than concentration, as these quantities are significantly different from each other over the range studied (activity coefficient close to 0.5). For all the experiments performed and re-analyzed, the activity coefficient for NH_4^+ and corresponding value of a_{NH4+} were calculated with the AIM model II (http://www.aim.env.uea.ac.uk/aim/model2/ model2a.php).[15] For instance, for the solutions $(NH_4)_2SO_4$ 0.1 M investigated experimentally in this work, a_{NH4+} = 0.12 M.

UV-Vis absorption analyses

For the UV-Vis analysis small samples (< 0.3 mL) of the reaction mixtures were placed in Quartz cells of pathlength, L = 1 mm and analyzed with an Agilent 8453 UV-Vis spectrometer, recording their absorbance, A_{10}, over 190 – 1100 nm. Taking samples at regular intervals allowed to follow the evolution of the absorbance of the mixture, and thus of the concentration of the compounds of interest, c, according to the Beer-Lambert law:

$$A_{10}(\lambda) = c \times \varepsilon_{10}(\lambda) \times L \qquad (1)$$

where λ is the wavelength (in cm), and $\varepsilon_{10}(\lambda)$ the absorption cross section or extinction coefficient of the compound in log 10 scale.

Table 1: List of the experiments performed in this work.

Analysis	Reagents, initial concentrations (M)
UV-Vis	G, 0.001
UV-Vis	G, 0.1
UV-Vis	Im, 0.005
UV-Vis	IC, 0.002
UV-Vis	BI, 0.0001
UV-Vis	Im, 0.01 + G, 0.005
UV-Vis	Im, 0.009 + G, 0.01
UV-Vis	Im, 0.005 + G, 0.01
UV-Vis	IC, 0.024 + G, 0.05
UV-Vis	IC, 0.008 + G, 0.005
UV-Vis	IC, 0.005 + G, 0.005
UV-Vis	BI, 0.002 + G, 0.003
UV-Vis	BI, 0.0001 + G, 0.001
^{1}H-NMR	G, 0.08
^{1}H-NMR	G, 0.08
^{1}H-NMR	Im, 0.034 + G, 0.01
^{1}H-NMR	Im, 0.026 + G, 0.005
^{1}H-NMR	IC, 0.014 + G, 0.013
^{1}H-NMR	IC, 0.009 + G, 0.004
^{1}H-NMR	BI, 0.0003 + G, 0.01
^{1}H-NMR	BI, 0.0004 + G, 0.009

^{1}H-NMR analyses

For the ^{1}H-NMR analysis, small samples of the 2-mL stirred reaction mixtures were taken and placed in 5-mm NMR tubes and in an AV500 Avance III Bruker spectrometer (500.13 MHz) equipped with 5 mm-BBI 1H/X and 5 mm-BBFO X/1H Z gradient probes. The spectra were recorded using the basic pulse zg sequence with 90° pulse excitation, a spectral width of 20 kHz, and an acquisition time of 3.2 s. The probes were tuned and calibrated with 90°-pulse on each sample. The relaxation times were evaluated and a delay of 60 s between pulse was found to be necessary to achieve the full relaxation of the products and reference.

The absolute quantification of the spectra was achieved with the BRUKER ERETIC2 module. Because the reactions studied were very slow and had to be monitored over several days, instrumental drift had to be compensated by using a reference. To avoid interactions with the reaction mixtures, an external reference was placed in a capillary, itself placed in the 5-mm tubes containing the reaction mixtures. This reference was a solution of tetradeuterated sodium trimethylsilylpropionate ($TSPD_4$) in D_2O of known concentration. The exact concentration of this reference solution under the conditions of the kinetic analyses was determined by placing it first in a 5-mm tube and measuring its concentration, C_{Ref}, with ERETIC2. This solution was then placed in a 1.7-mm capillary, itself placed in a 5-mm tube containing D_2O, and the ERETIC2 measurement gave a pseudo capillary concentration Cc_{Ref} related to the true concentration by the relationship $Cc_{Ref} = k_1 * C_{Ref}$ where $k_1 = V_{1.7mm}/V_{5mm}$. This factor k_1 was then used to quantify all the experimental spectra. As the signal for the reference is supposed to be

constant over the entire duration of the experiments, this correction allowed to compensate for long-term instrumental drift. A second correction was also applied to compensate for the smaller volumes of solution analyzed in the 5-mm tubes due to the presence of the capillary during the experiments. For this, ERETIC2 measurements were performed on a 5-mm tube containing a solution of known concentration, in the absence and in the presence of capillary. This provided the true concentration Ct, and the corrected concentration, Cc, respectively. The ratio k_2 = Ct/Cc was then applied to the ERETIC measurements obtained in the experiments to obtain the absolute concentrations in the reactions studied.

Finally, in order to quantify G in the experiments, although its chemical shift partly overlapped with the one of H_2O (see below), the reaction spectra were recorded at 283 K instead of room temperature. This temperature was however applied to the NMR tubes only during spectrum recording, which was a very short time compared to the duration of the experiment and did not affect the overall reaction kinetics.

The obtained spectra were processed with MestReNova software (Mestrelab Research). Prior to the experiments, the spectra of authentic standards for the compounds of interest were recorded in pure D_2O and in solutions $(NH_4)_2SO_4$ / D_2O 0.1 M at pH = 7 and 9, and gave the following characteristic shifts, δ_H (ppm): G, 4.8; Im, 7.24 (Ha) and 7.94 (Hb); IC, 7.44 (Ha) and 9.52 (Hb), and BI, 7.20 (Ha), formic acid, 8.3 - 8.4 These chemical shifts were used to identify these compounds in the experiments and follow their evolution. Note, however, that a small contamination resulting in an increase of formic acid during the experiments (up to 0.4 – 5 mM) precluded the use of this compound to characterize the reaction kinetics or yields.

Chemicals

Bis-2,2-1H-imidazole was synthesized for this study using the procedure described in ref.[13, 14] Its purity was determined by ^{1}H-NMR to be ≥ 99 %. All other compounds were purchased from Aldrich: Imidazole, 99%; imidazole carboxaldehyde, 99%; Glyoxal, aqueous solution 40 % wt. (8.8 M); ammonium sulfate, 99 %; D_2O, 99.9 atom % D; acetonitrile 99.8 %; trimethylsilyl propanoic acid (TMSP) 98 atom % D.

Results

UV-Vis absorption spectra and cross-sections of the imidazoles

The quantification of the molar yields for the imidazoles in the UV-Vis experiments required first to know their absorption spectra and extinction coefficients. The absorption spectra were obtained by dissolving the standard compounds in pure water and in solutions $(NH_4)_2SO_4$ / H_2O, 0.1 - 3 M. In pure water Im displayed a maximum absorbance at 205 nm, IC at 284 nm, with a weaker band at 214 nm, and BI at 275 nm (Figure 2). Note that, for IC and BI, these maxima are slightly different from those reported in the recent literature.[16, 17] In $(NH_4)_2SO_4$/H_2O solutions, the position of the main band for Im remained unchanged. But the one for IC shifted by about 4 nm towards the visible, thus to 288 nm. For BI, such a shift was observed only in 3 M solutions, to 278 nm.

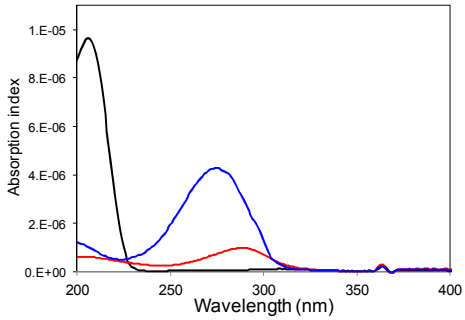

Figure 2: Absorption spectra for Im (black), IC (red) and BI (blue) in water.

Determining the extinction coefficients at these maxima was not straightforward because of the limited solubility of the imidazoles in aqueous solutions and the difficulty to know their dissolved concentrations. To overcome this problem all the solutions were subjected to ultrasounds for 20 min and the coefficients were determined by two independent approaches: 1) by measuring their UV-Vis absorbance in water/acetonitrile mixtures with increasing acetonitrile content: 0/100, 50/50, and 80/20 %; 2) by measuring, for the same solutions in D_2O, both the UV-Vis absorbance and the dissolved concentrations by ^{1}H-NMR. The results of these measurements and the recommended extinction coefficients are summarized in Table 2. The reported uncertainties include the repeatability of the measurements and the standard deviations in the linear regressions. For Im, both approaches provided similar extinction coefficients, which were also in good agreement with the literature.

Table 2: UV-Vis extinction coefficients for Im, IC, and BI obtained in this work, recommended values, and comparison with the literature.

Compound/ wavelength (nm)	conditions	ε_{10} (M^{-1} cm^{-1})	literature
Im / 205	H_2O	5119 ± 418	4571 ± 186[16] 4462 ± 245[17]
Im / 205	ACN/H_2O 50:50	4505 ± 30	
Im / 205	ACN/H_2O 80:20	4925 ± 418	
Im / 205	D_2O / ^{1}H-NMR	5000 ± 100	
Im / 205	**recommended**	**4728 ± 227**	
IC / 284	H_2O	9122 ± 229	230 ± 3[16] 273 ± 28[17]
IC / 284	ACN/H_2O 50:50	10897 ± 133	
IC / 284	ACN/H_2O 80:20	8704 ± 246	
IC / 284	D_2O / ^{1}H-NMR	13353 ± 300	
IC / 284	**recommended**	**10205 ± 2400**	
BI / 274	H_2O	2377 ± 201	36690 ± 998[17]
BI / 274	ACN/H_2O 50:50	13667 ± 152	
BI / 274	ACN/H_2O 80:20	18618 ± 960	
BI / 274	D_2O / ^{1}H-NMR	18778 ± 200	
BI / 274	D_2O/AS/ ^{1}H-NMR	18273 ± 200	
BI / 274	**recommended**	**17138 ± 2404**	

This was because Im is completely soluble in water, which was confirmed in our experiments by measuring dissolved concentrations with ^{1}H-NMR that were equal to the quantities initially introduced in solution (here, about 70 mM or 4.8 g L^{-1}). For IC at 284 nm, both approaches also resulted in similar extinction coefficients, giving confidence in the results. However, these coefficients were much larger than those reported in the literature. The NMR measurements showed that IC is less soluble than Im in water, the maximum dissolved concentration in D_2O being about 15 mM or 1.4 g L^{-1}. For BI at 274 nm, the obtained extinction coefficient increased with the acetonitrile fraction in the solvent, showing the better solubility of BI in organic solvents. The NMR measurements showed that the correct extinction coefficient was the one obtained with the highest acetonitrile content and the consistency between these two approaches gave confidence in the results. The NMR measurements gave a maximum dissolved concentration of BI in D_2O of 0.5 mM, or 0.07 g L^{-1}. The extinction coefficient obtained is, however, about 50 % lower than the one reported in the literature.

The positions and extinction coefficients for Im, IC and BI reported in this work are typical of $\pi \rightarrow \pi^*$ transitions of increasingly conjugated aromatic systems and thus, generally, supported by theory. In particular, the shift of the main band towards the visible from Im to IC, but to shorter wavelengths again from IC to BI, although the conjugated system becomes larger, can be explained by a simple particle-in-a-box approach. In this approximation, the difference in the transition wavelength between two systems, λ_1 and λ_2 (in nm), can be estimated from the relative length of their conjugated systems (L_1 and L_2, in Å), and the number of electrons involved (n_1 and n_2):

$$\left(\frac{n_2}{n_1} \times \frac{L_1}{L_2}\right)^2 = \frac{\lambda_1}{\lambda_2} \qquad (2).^{20}$$

From Im (n_1 = 6, λ_1 = 205 nm) to IC (n_2 = 8), the length of the conjugated system increases by about 50 % by adding the C-CH=O group to the imidazole ring. Thus, λ_2 (nm) ~ 205 / (8/6 x 0.64)^2 ~ 280 nm. From IC to BI, the length of the system increases by another 50 % by replacing the carbonyl group by a second imidazole ring but the number of electrons increases from n_2 = 8 to n_3 = 12. Thus, the transition is not shifted further towards the visible, but slightly back towards the UV, λ_3 (nm) ~ 284 / (12/8 x 0.68)^2 ~ 273 nm. Extinction coefficients are more difficult to predict than transition wavelengths. However those reported in this work are very similar to those of very similar molecules, where the imidazole aromatic ring is replaced by a C-6 ring: benzene (λ = 202 nm, ε = 7400 M^{-1} cm^{-1}), benzaldehyde (λ = 245 nm, ε = 10 000 M^{-1} cm^{-1}) and biphenyl (λ = 247 nm, ε = 16 000 M^{-1} cm^{-1}). All these fundamental arguments reinforce the confidence in our results.

Note that the extinction coefficient for Im obtained in this work allows also to refine the second-order rate constant for the self-reaction of glyoxal in ammonium salt solutions previously reported,[14] which was based on an approximate value of this coefficient. As this coefficient is found in this work to be about a factor 4 lower than the one assumed in this previous study, the previously reported rate constant needs to be lowered by the same factor.

Formation of imidazoles in the self-reaction of glyoxal

In this work, some experiments focused on the self-reaction of glyoxal in ammonium sulfate solutions, but exclusively to investigate the formation mechanism and yields for the imidazoles. As reported previously,[18] the UV-Vis spectra observed during this reaction (Figure 3A) displayed the formation of an intense band near 205 nm, corresponding to the formation of Im, and previously used to study the kinetics.[18] The formation of a smaller band near 289 nm was also observed, and corresponded to the formation of IC. The only other compound potentially contributing to these spectra was formic acid at 206 nm, the expected co-product of Im and directly overlapping with its absorption spectrum. But its contribution was estimated to be negligible because of its much smaller extinction coefficient than Im (39 M^{-1} cm^{-1}). The extinction coefficients recommended in Table 2 were used to quantify Im and IC in the reaction spectra and obtain time profiles for their concentrations.

This reaction was also studied by ^{1}H-NMR. This technique allowed to monitor the consumption of glyoxal at δ_H = 4.8 ppm. In addition, the formation of reaction products was observed. But, unlike in the cross-reactions presented below, the shifts were significantly displaced compared to those of the reference compounds.

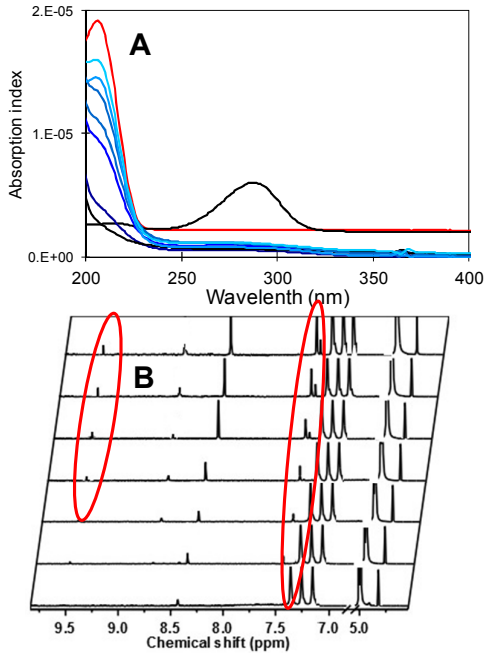

Figure 3: Evolution of the spectra during the self-reaction of G in aqueous ammonium sulfate solutions 0.1 M. (A) in UV-Vis absorption and comparison with reference spectra for Im (red) and IC (black); (B) in NMR, where the formation of Im and IC is evidenced by the peaks at 7.18 and 7.44 ppm, respectively.

Thus, the formation of Im was identified at δ_H = 7.46 ppm, and the one of IC at 7.42 and 9.50 ppm, which corresponded to the

shifts reported for these compounds in previous works.[16] The quantification of these peaks resulted in time profiles for all these compounds, which were used to determine the kinetics and yields.

Both in the experiments performed in this work and those re-analyzed, the quantity of Im produced in the self-reaction of G was much larger than that of IC. In the dilute salt solutions studied in this work, the ratio [Im]/[IC] was found to increase with reaction time, both in UV-Vis and ^{1}H-NMR (Figure 4). In the re-analyzed series of experiments, involving more concentrated salt solutions,[18] the ratio [Im]/[IC] also increased in the first part of the reaction but decreased at longer time (Figure 4), because of a further consumption of Im. These results clearly show that Im and IC are not co-products of the same reaction step but, rather, that Im is produced in first generation, while IC is produced in second generation. This conclusion will be confirmed by further experiments below.

The molar (or stoichiometric) yield for Im, Y_{Im}, in the self-reaction of G was determined from the time profiles obtained in this work by UV-Vis and NMR and by re-analyzing a series of about 70 experiments on the self-reaction of G, previously used to study the kinetics.[18] In most cases, Y_{Im} was determined by extrapolating to t = 0 the time evolution of the ratio:

$$Y_{Im}(t) = \frac{[Im]_t}{[G]_o - [G]_t} \qquad (3),$$

where $[Im]_t$ and $[G]_t$ are the concentrations of Im and G at time t of the experiment. In ^{1}H-NMR, where both Im and G were monitored, $Y_{Im}(t)$ was determined directly. In the UV-Vis experiments, where G was not monitored, Y_{Im} was determined either by extrapolating Eq. (2) to t = 0, where the decay of G was estimated from the rate constant previously published,[18] or from the ratio $[Im]_t/[G]_o$ at large conversion of G, assuming a total consumption of G. Whenever possible, both methods were compared and gave the same results. The values of Y_{Im} thus obtained over $[G]_o$ = 0.001 – 0.5 M, a_{NH4+} = 0.1 – 8 M, and pH = 5 – 9 are presented in Figure 5. The uncertainties and dispersion in the data are due to the uncertainties in extrapolating $Y_{Im}(t)$ to t = 0 and in estimating the decay of G in UV-Vis. It is clear in Figure 5A that Y_{Im} varies strongly with $[G]_o$.

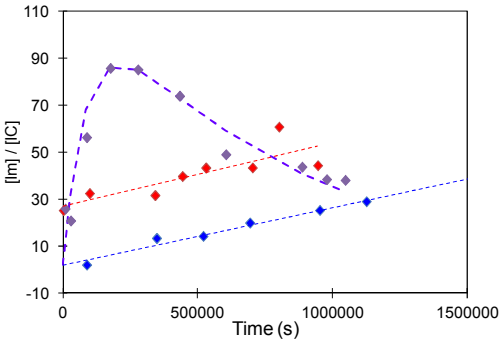

Figure 4: Ratio [Im] / [IC] in the self-reaction of glyoxal in aqueous ammonium salt solutions. Red symbols: in solution 0.1 M observed by UV-Vis; Blue symbols: in 0.1 M solutions observed by 1H-NMR; Purple symbols: in 2.6 M solution observed by UV-Vis.

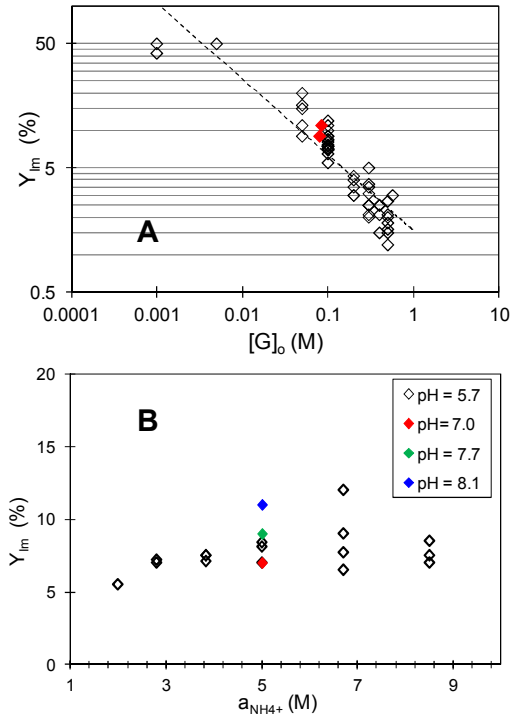

Figure 5: Values of Y_{Im} in the self-reaction of G, obtained in the experiments of this work and in the re-analysis of previous experiments. (A): as function of $[G]_o$ and over a wide range of aqueous ammonium sulfate solutions, measured by UV-Vis (black symbols) and by NMR (red symbols); (B): as function of a_{NH4+} and pH for $[G]_o$ = 0.1 M.

The slope of the line obtained in a ln-ln scale was – (0.89 ± 0.24), indicating that, within uncertainties, Y_{Im} varies inversely with $[G]_o$. The large uncertainties (± 50 %) on this slope at the lowest values for $[G]_o$ result from the larger experimental uncertainties on the volumes of G injected in the reaction mixtures. The inverse variation of Y_{Im} with $[G]_o$ was attributed to the kinetic competition between the imidazole-producing condensation channel of the self-reaction and the catalytic channel producing acetals and oligomers.[18]

However, within the uncertainties, Y_{Im} did not vary with other experimental parameters such as a_{NH4+}, and pH (Figure 5B). As these parameters are known to strongly affect the reaction kinetics,[16, 18] this implies that both the catalytic and the non-catalytic channels of the self-reaction of glyoxal are equally affected by a_{NH4+} and pH. This, in turn, suggests that they are both kinetically limited by the formation of a common reaction intermediate.

The analysis of the time profiles also allowed to determine the kinetics of the self-reaction of G at low ammonium concentration. The kinetics of this reaction has been extensively studied previously, but mostly in concentrated ammonium salt solutions (a_{NH4+} = 2 – 8 M), where the rate is second order in G. But for $a_{NH4+} \leq 2$ M, it was reported to be first order in G,[18] with a first-order rate constant of k^I_{G+G} (s^{-1}). The experiments performed in this work allowed to further study k^I_{G+G} at low ammonium concentrations (a_{NH4+} = 0.12 M) and to investigate its variations with catalyst activity, a_{NH4+}.

The value of the rate constant k^{I}_{G+G} measured in this work with a_{NH4+} = 0.12 M was $k^{I}_{G+G} = (1.4 \pm 0.9) \times 10^{-7}$ s^{-1}.

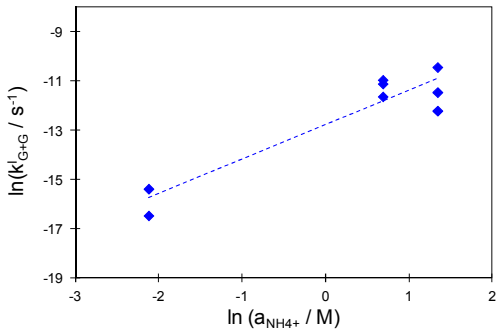

Figure 6: Variations of the first-order rate for the self-reaction of G, k^{I}_{G+G}, as function of a_{NH4+} at low NH_4^+ concentration.

Putting together the values of k^{I}_{G+G} obtained in this work and those from the re-analyzed experiments with $a_{NH4+} \leq 2$ M in a ln-ln scale gave a line of slope (1.4 ± 0.7) (Figure 6), showing that, over the range a_{NH4+} = 0.12 – 2, M k^{I}_{G+G} varies as a first order in a_{NH4+}: k^{I} (s^{-1}) = $k^{II} \times a_{NH4+}$, with $k^{II} = (7.8 \pm 2.5) \times 10^{-6}$ s^{-1} M^{-1}.

Cross-reaction between Im and G

The concentration of Im alone in aqueous ammonium sulfate solutions monitored by UV-Vis did not display any decay over the typical timescale studied in this work (0 - 900 h).

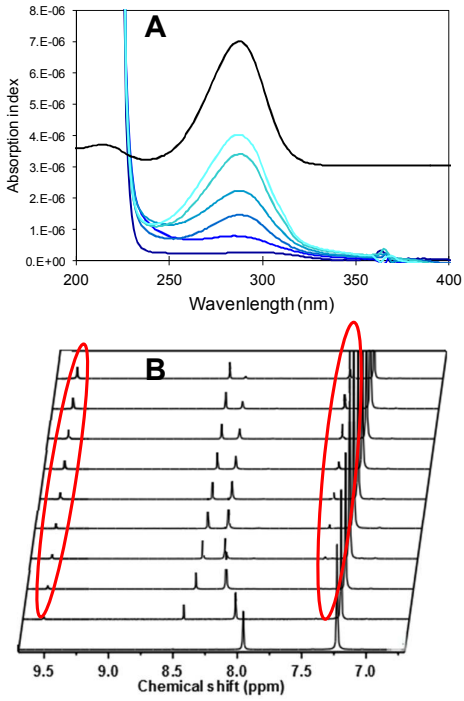

Figure 7: Evolution of the spectra during the cross-reaction between Im and G in aqueous ammonium solutions 0.1 M at pH = 7. (A) in UV-Vis, with comparison with the reference spectrum for IC (black curve); (B) in NMR, where the peaks at 7.44 and 9.5 ppm evidence the formation of IC.

It was thus concluded that Im does not undergo any significant reaction under these conditions.

The cross-reactions between Im and G was studied both by UV-Vis absorption and NMR (Table 1). The evolution of the spectra of the reaction mixtures in this reaction are illustrated in Figure 7. In the UV-Vis experiments, where only Im and IC were monitored, the formation of IC was evidenced by the formation of an absorption band at 288 nm (Figure 7A). In the NMR experiments, where all the compounds could be monitored, reaction products were unambiguously identified by comparison of their chemical shift with those of the reference compounds reported above. Thus, the formation of IC was evidenced by the formation of a peak at δ_H = 7.44 and 9.52 ppm (Figure 7B).

The time profiles obtained in UV-Vis and by NMR in these experiments allowed to study the kinetics of this cross-reaction and to determine the yield for IC, Y_{IC}. This yield was obtained by extrapolating to t = 0 the following ratios:

$$Y_{IC}(t) = \frac{[IC]_t}{[G]_o - [G]_t} = \frac{[IC]_t}{[Im]_o - [Im]_t}, \qquad (4)$$

where $[IC]_t$ is the concentrations of IC at reaction time t, and $[Im]_o$ the concentration of Im initially introduced in the mixture. In UV-Vis, where G was not monitored, only the expression on the right hand side could be used. In NMR both expressions could be used and their results were compared. In all cases, the decays of G and Im had to be corrected for the contribution of the self-reaction of G. In the NMR analyses, the overall decay of G was corrected for k^{I}_{G+G}. And both in the UV-Vis and NMR experiments, the decays of Im had to be corrected for its formation by the self-reaction of G, using the rate constants reported previously and the values of Y_{Im} reported in this work. The time evolution of $Y_{IC}(t)$ in these experiments and their extrapolation to t = 0 are shown in Figure 8. The uncertainties are due to the corrections for the self-reaction of G. As shown in Figure 8 $Y_{IC}(t)$ decreased strongly with reaction time because of the further reaction of IC in the mixtures. In spite of the uncertainties, extrapolating $Y_{IC}(t)$ to t = 0, gave values for Y_{IC} close to unity (0.93 ± 0.22).

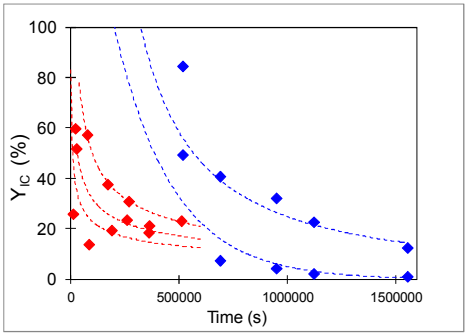

Figure 8: Determination of Y_{IC} in the cross-reaction between Im and G by UV-Vis absorption (red symbols) and ^{1}H-NMR experiments (blue symbols). Dashed lines are the extrapolations to t = 0.

These results confirmed that IC is quantitatively produced by the cross-reaction between Im and G in aqueous ammonium

solutions. Thus, the IC observed in reaction mixtures starting from G must have been produced by the further reaction of the Im produced in first generation with G, thus in second generation from G.

The time profiles obtained in UV-Vis and NMR also allowed to estimate the first-order rate for the cross-reaction between Im and G, k^{I}_{Im+G}, under the conditions studied in this work (a_{NH4+} = 0.12 M, $[G]_o$ = 3.5-8 mM): $k^{I}_{G+Im} = (2.5 \pm 1.5) \times 10^{-7}$ s^{-1}.

Cross-reaction between IC and G

The time evolution of IC alone in aqueous ammonium sulfate solutions monitored in UV-Vis displayed a decrease corresponding to a first-order rate of 1×10^{-7} s^{-1}. The process or reaction responsible for this decay was however not identified.

The cross-reaction between IC and G was also studied by UV-Vis and NMR. The evolution of the spectra in NMR unambiguously evidenced the formation of BI by the formation of a peak at the characteristic shifts δ_H = 7.20 ppm, in agreement with the spectrum of the corresponding reference compound (Figure 9B). The presence of two other unidentified peaks was also observed at 7.31 and 7.39 ppm. The NMR spectra provided time-evolution for all the compounds involved, G, IC, and BI.

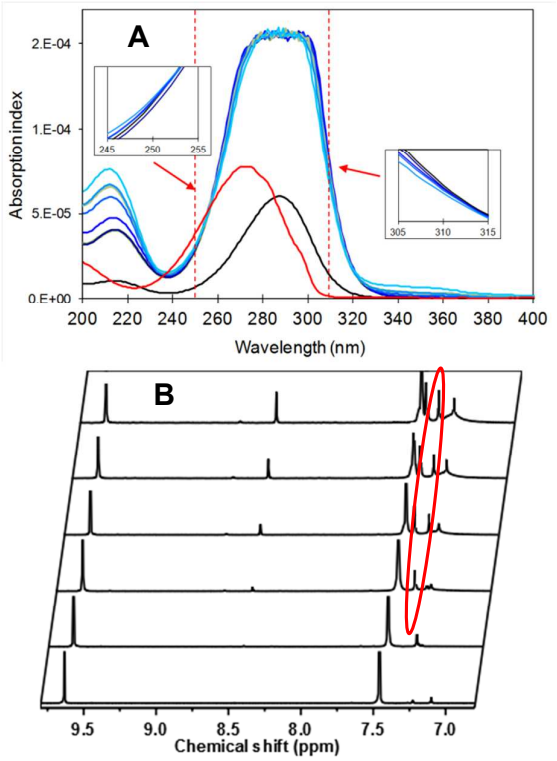

Figure 9: Evolution of the spectra in the reaction between IC and G in aqueous ammonium sulfate solutions 0.I M at pH = 7. (A) in UV-Vis and comparison with reference spectra for IC (black) and BI (red). The red dashed lines are the wavelengths used to quantify BI and IC ; (B) NMR spectra for the same reaction evidencing the formation of BI at 7.19 ppm.

In UV-Vis, because of the partial overlap of the main bands for IC and BI, the formation of BI resulted in an apparent broadening of the main absorption band at 240 - 320 nm (Figure 9A). The concentrations and time profiles for IC and BI could however be retrieved from these spectra by measuring the absorbance at wavelengths that avoided the overlap: 250 nm for BI and 310 nm for IC (see details in Figure 9A).

The time profiles obtained in NMR and UV-Vis were analyzed to determine the yield of BI in the cross-reaction between IC and G, Y_{BI}. This yield was determined by extrapolating to t = 0 the following ratios:

$$Y_{BI}(t) = \frac{[BI]_t}{[G]_o - [G]_t} = \frac{[BI]_t}{[IC]_o - [IC]_t} \quad (5),$$

where $[IC]_O$ is the concentration of IC initially introduced. In the NMR experiments, Y_{BI} could be determined directly by the left hand side expression of the ratio, where the concentration of G was corrected to account for its self-reaction. Both in NMR and in UV-Vis, the right hand side expression for Y_{IC} was also estimated, where $[IC]_t$ was corrected for the decay observed for IC alone in ammonium sulfate solutions. The results are presented in Figure 10. Both in NMR and in UV-Vis, the extrapolations to t = 0 led to a value of Y_{IC} close to unity (0.95 ± 0.23).

These results show that BI is quantitatively produced by the cross reaction between G and IC. Thus, the BI found previously in reaction mixtures starting from G only must have been produced from the further reactions of IM and IC with G, thus as a third-generation product from G.

The time-profiles obtained from the experiments also allowed to estimate a first-order rate for the cross-reaction of IC and G under these conditions (a_{NH4+} = 0.12 M), $k^{I}_{IC+G} = (6.3 \pm 3.6) \times 10^{-7}$ s^{-1}.

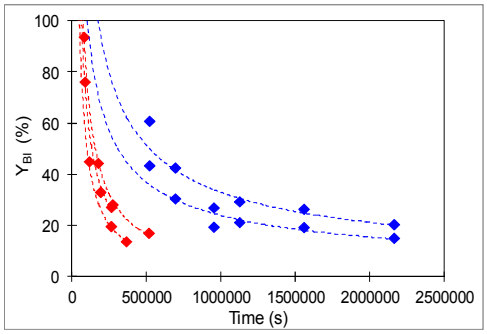

Figure 10: Determination of YBI in the cross-reaction between IC and G in aqueous ammonium solutions 0.1 M observed in UV-Vis absorption (red symbols) and ^{1}H-NMR experiments (blue symbols). Dashed lines are the extrapolations to t = 0.

Cross-reaction between BI and G

The time evolution of BI alone in aqueous ammonium salt solutions displayed a constant increase over the typical timescale studied, which was equivalent to a first-order formation rate of $k^{I}_{BI} \sim 1 \times 10^{-7}$ s^{-1}. The reason for this increase was unclear but attributed to the slow dissolution of this compound in aqueous solutions.

The cross-reaction between G and BI in aqueous ammonium sulfate solutions was also studied. The formation of new absorption bands in UV-Vis, resulting in a apparent shift of the initial band of BI from 278 to 285 nm showed that a reaction was taking place (Figure 11A). Subtracting the reference spectrum for BI from the reaction spectra evidenced the formation of new bands at 295 nm, and possibly at 311 nm (Figure 11B). The occurrence of a reaction between BI and G and the formation of products was also confirmed in NMR, by the formation of new peaks at chemical shifts δ_H = 7.24 and 7.45 ppm (Figure 11C). Assuming the same number of proton than BI, the product at 7.24 ppm accounted for nearly 100 % of conversion of BI. But because of the complexity of the reaction spectra, these products could not be identified. They are, however, likely to correspond to the absorption bands observed at 295 and 311 nm in UV-Vis.

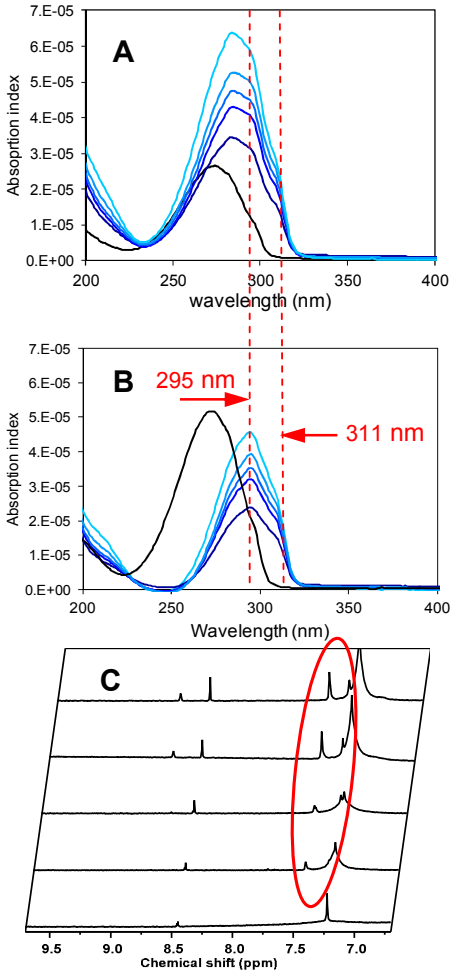

Figure 11: Evolution of the spectra evidencing a reaction between BI and G in aqueous ammonium sulfate solution 0.1 M at pH = 7. (A) Overall UV-Vis spectra; (B) UV-Vis spectra after subtraction of the reference spectrum for BI (black curve) evidencing reaction products absorbing at 295 and 311 nm; (C) NMR spectra evidencing reaction products at 7.4 and 8.6 ppm.

The constant increase of BI in these experiments, due to its slow dissolution, and the contribution of the self-reaction of G precluded an accurate analysis of the kinetics of the cross reaction.

Discussion and conclusion

Formation mechanisms for Im, IC, and BI and implications for their synthesis. By investigating separately the self-reaction of G and each of its cross-reactions with Im, IC, and BI, this study clearly demonstrated that only Im is significantly produced in the self-reaction of G, and that IC and BI result quantitatively from its cross-reactions with Im, and IC, respectively, thus in second and third generation from G. Even by studying these reactions step-by-step the analyses were not straightforward because of the contributions of self-reactions and other processes to the cross-reactions. Obtaining such mechanistic information from more complex systems or when starting from G only would therefore be nearly-impossible.

The sequence of reactions producing Im, IC, and BI from G and deducted from the results of this work is summarized in Figure 12. In this sequence, the maximum possible stoichiometric (or molar) yields for the imidazoles relative to G are Y_{Im} = 0.5, Y_{IC} = 0.33, and Y_{BI} = 0.25.

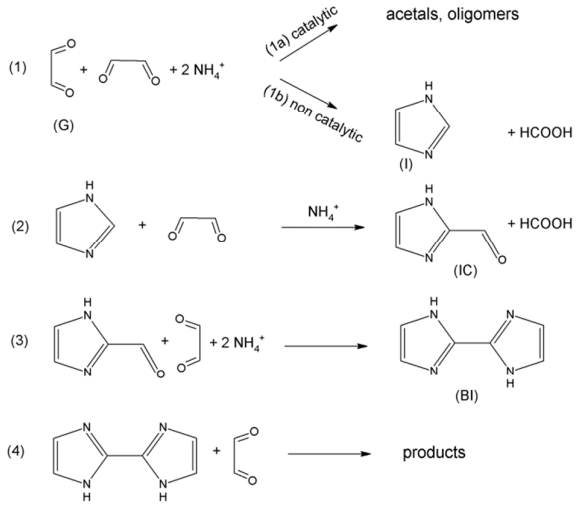

Figure 12: Reaction sequence explaining the successive formation of Im, IC, and BI in mixtures of glyoxal in aqueous inorganic ammonium salt solutions, proposed based on the results of this work.

However, the results of this work show that, while Y_{IC} and Y_{BI} in the cross-reactions where close to unity, Y_{Im} in the self-reaction of G was small and strongly dependent on $[G]_o$, which was attributed to the competition between the Im-producing channel and the acetal/oligomer-producing channel of this reaction under the neutral and aqueous conditions studied. This first step represents therefore the main bottleneck for the formation of larger imidazoles from G. On the other hands, the results of this work demonstrate that the production of significant yields of Im or larger imidazoles is possible under environmentally-friendly aqueous and neutral conditions, provided that $[G]_o$ is maintained below 0.1 M. Although this condition might appear as a hindrance to large-scale

production, it can be overcome in open/flow systems, where G is added progressively, and potentially lead to significant amounts of imidazoles. Working at pH = 7 in this work should have limited the importance of the acetal-forming channel compared to acidic or basic conditions, and its competition with the imidazole-producing channel. But the formation of acetals in aqueous mixtures could be further lowered by increasing the temperature, which should provide even better imidazole yields for moderate or high concentrations of G than reported in this work. Starting from larger carbonyl compounds, such as methylglyoxal, aldehydes or ketones, under similar neutral and aqueous solutions should also give much better imidazole yields, regardless of the initial carbonyl concentration, because the smaller importance of the acetal-forming channel for such compounds.

Implications for the formation of light-absorbing compounds in atmospheric aerosols. In addition to their synthetic interest, the formation of imidazoles from the reactions of G in aqueous ammonium solutions was studied in this work because of their potential interest as markers for the reaction of G with NH_{4+} in atmospheric aerosols. These reactions also illustrate the production of light-absorbing compounds from simple precursors, which are important for the optical properties of atmospheric aerosols.[15, 16, 21-27] In the last few years, the reaction of other carbonyl compounds with NH_4^+ have also been shown to produce light-absorbing products, some absorbing as far in the visible as 500 nm.[21, 26-30] The results of this work show that the formation of such conjugated products in atmospheric aerosols would not be limited to single steps but proceed in successive steps producing compounds absorbing further and further in the visible and having increasingly large extinction coefficients. The importance of such reactions and products in atmospheric aerosols remains largely to be explored.

Acknowledgements

Neda Nikoobakht, now at the University of Manitoba, Canada, is gratefully acknowledged for the synthesis of 2,2-bis-1H-imidazole. A. Maxut is funded by a grant from the French Minister for Higher Education and Research.

Notes and references

1. J. C. Lee, J. T. Laydon, P. C. McDonnell, T. F. Gallagher, S. Kumar, D. Green, D. McNulty, M. J. Blumenthal, J. R. Keys, S. W. Land vatter, J. E. Strickler, M. M. McLaughlin, I. R. Siemens, S. M. Fisher, G. P. Livi, J. R. White, J. L. Adams and P. R. Young, *Nature*, 1994, **372**, 739.
2. L. Wang, K. W. Woods, Q. Li, K. J. Barr, R. W. McCroskey, S. M. Hannick, L. Gherke, R. B. Credo, Y.-H. Hui, K. Marsh, R. Warner, J. Y. Lee, N. Zielinski-Mozng, D. Frost, S. H. Rosenberg and H. L. Sham, *J. Med. Chem.*, 2002, **45**, 1697.
3. T. Welton, *Chem. Rev.*, 1999, **99**, 2071.
4. J. P. Hallett and T. Welton, *Chem. Rev.*, 2011, **111**, 3508.
5. R. J. Sundberg and R. B. Martin, *Chem. Rev.*, 1974, **74**, 471.
6. S. H. Seo, J. H. Park, G. N. Tew and J. Y. Chang, *Tetrahedron Lett.*, 2007, **48**, 6839.
7. M. Wächtler, S. Kupfer, J. Guthmuller, S. Rau, L. González and B. Dietzek, *J. Phys. Chem. C*, 2012, **116**, 25664.
8. S. H. Seo and J. Y. Chang, *Chem. Mater.*, 2005, **17**, 3249.
9. S. H. Seo, G. N. Tew and J. Y. Chang, *Soft Matter*, 2006, **2**, 886.
10. H. Debus, *Justus Liebigs Annalen der Chemie*, 1858, **107**, 199.
11. B. Radzisewski, *Berichte der deutschen chemischen Gesellschaft*, 1882, **15**, 2706.
12. B. F. Fieselmann, D. N. Hendrickson and G. D. Stucky, *Inorg. Chem.*, 1978, **17**, 2078.
13. F. Mao, N. Mano and A. Heller, *J. Am. Chem. Soc.*, 2003, **125**, 4951.
14. *USA Pat.,* US 6,713,631 B2, 2004.
15. M. M. Galloway, P. S. Chhabra, A. W. H. Chan, J. D. Surratt, R. C. Flagan, J. H. Seinfeld and F. N. Keutsch, *Atmos. Chem. Phys.*, 2009, **9**, 3331.
16. G. Yu, A. R. Bayer, M. M. Galloway, K. J. Korshavn, C. G. Fry and F. N. Keutsch, *Environ. Sci. Technol.*, 2011, **45**, 6336.
17. C. J. Kampf, R. Jakob and T. Hoffmann, *Atmos. Chem. Phys.*, 2012, **12**, 6323.
18. B. Nozière, P. Dziedzic and A. Córdova, *J. Phys. Chem. A*, 2009, **113**, 231.
19. N. Sedehi, H. Takano, V. A. Blasic, K. A. Sullivan and D. O. De Haan, *Atmos. Environ.*, 2013, **77**, 656.
20. D. A. McQuarrie, University Science Books, Davis, USA, 2007.
21. E. L. Shapiro, J. Szprengiel, N. Sareen, C. N. Jen, M. R. Giordano and V. F. McNeill, *Atmos. Chem. Phys.*, 2009, **9**, 2289.
22. N. Sareen, A. N. Schwier, E. L. Shapiro, D. Mitroo and V. F. McNeill, *Atmos. Chem. Phys.*, 2010, **10**, 997.
23. M. Trainic, A. Abo Riziq, A. Lavi, J. M. Flores and Y. Rudich, *Atmos. Chem. Phys.*, 2011, **11**, 9697.
24. A. K. Y. Lee, R. Zhao, R. Li, J. Liggio, S.-M. Li and J. P. D. Abbatt, *Environ. Sci. Technol.*, 2013, **47**, 12819.
25. M. H. Powelson, B. M. Espelien, L. N. Hawkins, M. M. Galloway and D. O. De Haan, *Environ. Sci. Technol.*, 2014, **48**, 985.
26. B. Nozière, M. Kalberer, M. Claeys, J. Allan, B. D'Anna, S. Decesari, E. Finessi, M. Glasius, I. Grgić, J. F. Hamilton, T. Hoffmann, Y. Iinuma, M. Jaoui, A. Kahnt, C. J. Kampf, I. Kourtchev, W. Maenhaut, N. Marsden, S. Saarikoski, J. Schnelle-Kreis, J. D. Surratt, S. Szidat, R. Szmigielski and A. Wisthaler, *Chem. Rev.*, 2015, DOI: 10.1021/cr5003485.
27. A. Laskin, J. Laskin and S. A. Nizkorodov, *Chem. Rev.*, 2015, DOI: 10.1021/cr5006167.
28. D. L. Bones, D. K. Henricksen, S. A. Mang, M. Gonsior, A. P. Bateman, T. B. Nguyen, W. J. Cooper and S. A. Nizkorodov, *J. Geophys. Res.*, 2010, **115**, D05203.
29. K. M. Updyke, T. B. Nguyen and S. A. Nizkorodov, *Atmos. Environ.*, 2012, **63**, 22.
30. T. B. Nguyen, A. Laskin, J. Laskin and S. A. Nizkorodov, *Faraday Discuss.*, 2013, **165**, 473.